FACTA UNIVERSITATIS
Series: **Mechanical Engineering**
https://doi.org/10.22190/FUME240730043G

Original scientific paper

USE OF FIVE-PARAMETER OPTIMIZATION OF ATTACHMENT LUG GEOMETRY TO IMPROVE ITS FATIGUE LIFE

Vanja Stefanović Gobeljić[1], Aleksandar Grbović[2], Aleksandar Sedmak[2], Simon Sedmak[3], Gordana Djukanovic[4], Aleksandar Bogojević[5], Ivana Vučetić[3]

[1]Military Technical Institute, Belgrade, Serbia
[2]Faculty of Mechanical Engineering, University of Belgrade, Serbia
[3]Innovation center of the Faculty of Mechanical Engineering, Belgrade, Serbia
[4]Faculty of Forestry, University of Belgrade, Serbia
[5]University of Belgrade, Institute of Physics, Belgrade, Serbia

Abstract. *Pin-loaded attachment lugs are highly loaded and responsible aircraft component prone to fatigue failure. Thus, here the geometry of the wing-fuselage attachment lug was optimized using the fatigue life as the criterion. Separating Morphing and Adaptive Remeshing Technology (SMART) was used in the scope of Finite Element Method (FEM) to simulate fatigue crack growth by and to obtain fatigue life for different geometry parameters. Five-parameter optimization was applied, by varying two radii (rounding radius and radius of a pin hole), "hump" parameter, outer radius and thickness, using five different models. It was shown that fatigue life can be significantly improved with only modest increase of mass.*

Key words: *Optimization, Attachment lug, SMART FEM, Fatigue crack growth*

1. INTRODUCTION

The wing spar is connected to the aircraft fuselage by so-called aircraft fittings with attachment lug as the crucial component, Fig. 1. Needless to say, eventual failure of such a component leads to inevitable aircraft loss, [1]. One should notice that attachment lugs are designed as safe-life components, [2], so experimental verification of their fatigue life is not required by regulations. Yet, many recent events indicate unexpected damages in attachment lugs, including fatigue cracks, [3]. As an example, cracks were found in Boeing 737NG pickle

Received: July 30, 2024 / Accepted October 02, 2024
Corresponding author: Simon Sedmak
Innovation center of the Faculty of Mechanical Engineering, Belgrade, Kraljice Marije 16, 11000 Belgrade, Serbia
ssedmak@mas.bg.ac.rs

forks after shorter period of time then mandatory inspection period, [3], forcing airlines to make additional monitoring. As a consequence, about 50 jets were grounded worldwide to find a way to prevent fatigue crack initiation and growth, [3-4]. In this way, a new concept was introduced, based on fail-safe design, which includes possibility of crack growth and procedure how to deal with it, contrary to the safe-life design approach, [5-6]. In other words, even though the safe-life design approach tends to be overconservative, it does not guarantee the safety, so here the fail-safe approach will be considered, to accommodate the fact that cracks are often inevitable and controllable. Toward this aim one should consider region around attachment lug hole, since this is the location of the highest stresses.

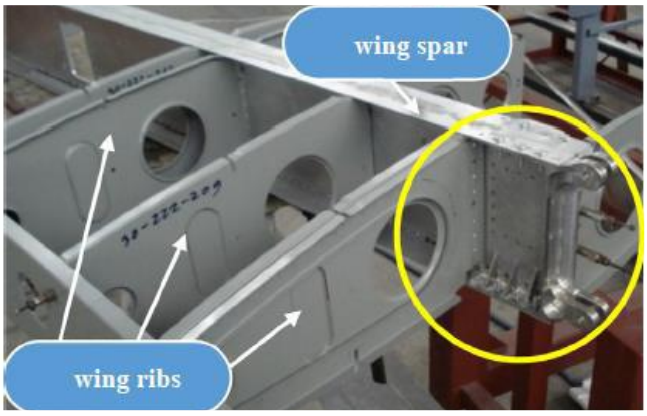

Fig. 1 Light aircraft wing-fuselage attachment (circled) with two pairs of lugs, [6]

Fatigue behaviour of different types of aircraft attachment lugs and fittings was analysed recently, as described in the following text.

Failure of two trailing-edge flap (TEF) hinge lugs was attributed to large fatigue cracks found around the bearing hole, [7]. Cracks were initiated by extensive pitting corrosion, as well as fretting in one case. Crack growth rate was about 10 times higher than the manufacturer predicted. Another example of corrosion related damage initiating fatigue failure of a wing-fuselage link was analysed in [8]. It was concluded that the failure was the combination of fatigue and corrosion, as well as the consequence of high stresses in the wing lug area.

Fatigue failure of an aircraft landing gear due to the outer cylinder lug fracture was investigated in [9], indicating both stable and unstable crack growth due to specific microstructure orientation. The most probable cause of this failure was a combination of corrosion cavities and the high landing loads in a critical area. Another failure analysis, [10], was focused on the effect of the lug head, introducing model for estimation of fatigue strength of pin-loaded lug with through-the-thickness crack. Results were verified by the experimental ones.

Constant amplitude loading was used in [11] to validate the NASGRO 4 fatigue crack growth rate data, and to simulate real aircraft joint behaviour. Faster crack growth was found in the lug surface direction contrary to previous results which had indicated faster growth in thickness direction. In [12], straight attachment lug under oblique loading (maximum 45^{o})

was analysed using ANSYS, to study effects of crack length, radius ratio, and pin-load angle (β) on the SIFs values.

Two different material combinations for wing-fuselage lug attachment bracket (steel AISI 4340 and AA 2024 T351 in the first case, and titanium alloy Ti6Al4V and AA 7075 T6 in the second one) were studied in [13] by numerical simulation. The second combination of materials enabled reduction of total weight of the brackets from 36.8 kg to 24.4 kg.

Extensive study by MSC Patran/Nastran, presented in [14], provided the maximum tensile stress location in a pin-loaded lug. This study proved that the decreasing radius ratio increases stress concentration factor, thus reducing the maximum number of cycles to failure.

Stress intensity factors for single and elliptical cracks were evaluated by 3D boundary element method for different crack length and radius ratios to estimate fatigue life of attachment lug, [15]. Similar approach was used in [16] to prove that numerical simulation of fatigue crack growth through the thickness is in agreement with the experimental results. Studies [17-19] verified numerical simulation results by comparison with analytical and/or experimental results for a cracked pin-loaded lug under cyclic loading with either constant amplitude or an overload. The effect of width, hole diameter and thickness on the lug strength was assessed. In particular, the residual life of an attachment lug was estimated in [19], using finite element modelling compared with analytical expressions for stress intensity factors. Similar approach was applied in this paper.

Similar to the previous three studies, analytical models were used for calculation of stress distribution in a lug, [20], and results were verified by FEM. Computational model was introduced in [21] to analyse the crack growth in attachment lugs with different cracks by using ANSYS with 4-noded finite element. Numerical results were verified by the experimental data, as well as with analytical expressions for FCG, encouraging further efforts in this direction, as shown here. Similar problem was tackled in [22] by applying 3D extended version of FEM (XFEM, as built in ABAQUS), Two different load ratios were used (0.1 and 0.5) indicating significant effect of different loading boundary conditions on the estimated fatigue life.

To summarize briefly, numerical and analytical tools are nowadays available as powerful and reliable tools for residual life evaluation of critical components with complex geometry, such as attachment lug. In this paper numerical simulation of fatigue crack growth in a connection lug is used to make Five-parameter optimization of an attachment lug geometry. Some aspects of this study were already considered [23-26]. Solob et al., [23], used both extended finite element method (XFEM) and classical FEM with Separating Morphing and Adaptive Remeshing Technology (SMART) to calculate SIFs for fatigue crack in attachment lug of a light aerobatic aircraft and to estimate resulting remaining fatigue life. In the scope of XFEM analysis, growth of a penny-shaped corner crack was compared with the growth of through-the-thickness crack, located at the same position, to calculate number of cycles to complete failure confirming the fact that the actual attachment lugs must be redesigned using a fail-safe approach. Afterwards, through-the-thickness crack was analysed also with classical FEM using SMART, as built in ANSYS. These two techniques were compared, indicating higher SIF values obtained by XFEM and thus the shorter fatigue life, [23]. Grbovic et al., [24], used two-parameter optimization (thickness, hole radius) to get the optimal geometry of the wing-fuselage attachment by using the fatigue life as the criterion. Toward this aim numerical simulation of fatigue crack growth by XFEM and SMART was used to obtain

fatigue life for different geometry parameters. In the meantime, experimental verification of numerical results was carried out on the full-scale wing, [25], indicating good agreement for calculated and measured strains and confirming that loads acting on the wing-fuselage attachment lug were accurately evaluated. Finally, in the recently published review paper, [26], some of the results were reconsidered and analyzed in more details. One should notice that contrary to the XFEM, which uses the same mesh through the simulation, crack front mesh adapts with every growth step when SMART FEM is used, [26]. The latter option is applied here, as provided by ANSYS, using tetrahedral elements.

In this paper five-parameter optimization is presented (thickness, rounding radius and radius of a pin hole, "hump" parameter and outer radius) with the goal to prolong fatigue life of lug without excessive increase of mass (fail-safe approach) and to prevent its premature failure in this way.

2. NUMERICAL SIMULATION

Numerical simulation of the fatigue crack growth is commonly based on the use of XFEM, [26-28], or, more recently, on the application the Separating Morphing and Adaptive Remeshing Technology (SMART) in the scope of classical FEM, [29]. Both methods were used recently to solve different problems, such as fatigue crack growth in standard Charpy specimen, [30], and remaining life of cracked welded joints, [31].

FEM model, including boundary and loading conditions, is shown in Fig. 2, indicating fixed points (in pink color) at the bottom surface and loading area in the upper surface (in red color). More details, including finite element mesh effects, are presented in [6].

In respect to the amplitude loading, stress ratio R=−1 was used as a representative of real wing load. As for the material, Paris coefficients n=2.26 and C=7.526·10^{-11} were adopted from ANSYS data base, [29], for the high strength steel used in this case, [6]. Finite element mesh with an average element mesh size of 1.7 mm is shown in Fig. 3. Stress Intensity Factor (SIF) values after the first crack growth step are shown in Fig. 4, indicating K_{Imax} = 1880 MPa√mm, and all the values of K_I along the crack front to be in-between 1850 and 1880 MPa√mm, [24].

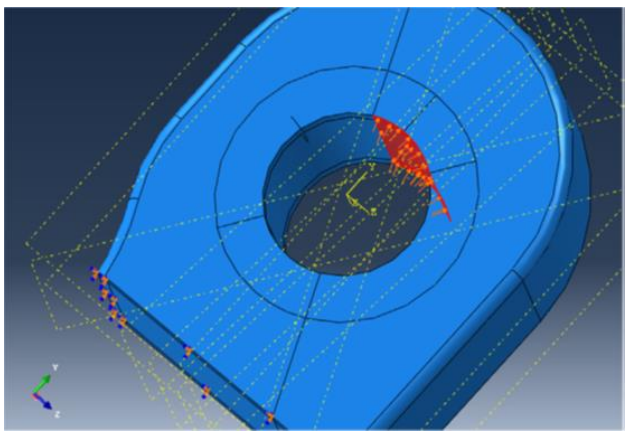

Fig. 2 Finite element model of attachment lug, [32]

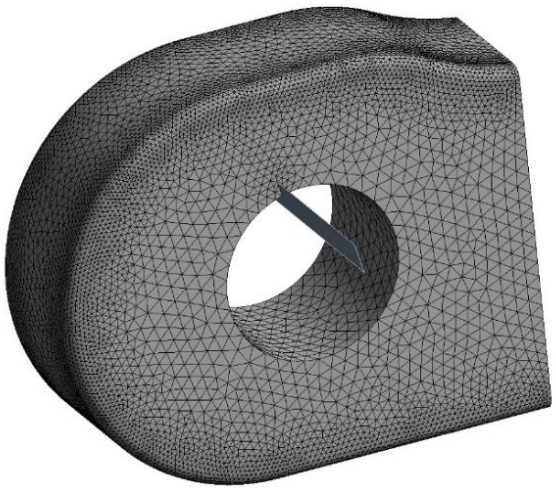

Fig. 3 Finite element mesh used in optimization

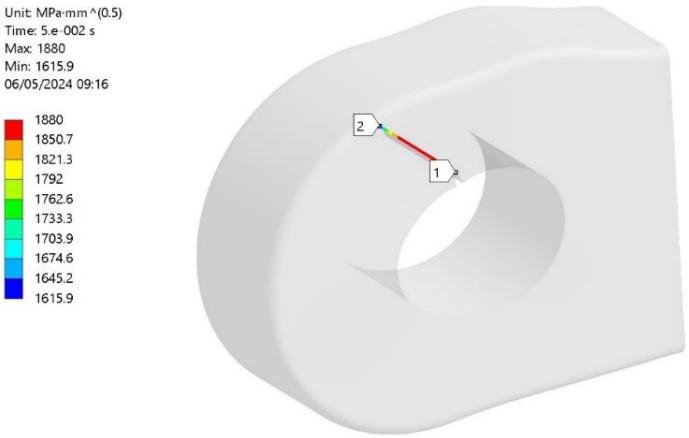

Fig. 4 SIF values along crack front after 1st step of propagation (original lug)

3. OPTIMIZATION

For the optimization purposes it was required to reduce K_{Imax} after the first crack growth step, if possible, as explained in [24]. Another optimization criterion was to keep the mass of the attachment lug as close as the initial value (87 grams), [6].

The first step in the optimization process was to model increasing thickness. In this way, number of cycles was increased to N_{max}=1085 (thickness 17 mm), i.e. more than doubled in respect to the original one (N_{max}=515 for thickness 12 mm). More detailed results are shown in [24, 32]. The next step was two-parameter optimization, with thickness and radius of the surface varied. In the case the thickness 17 mm and rounding radius 19 mm, SIF values along the crack front for lug were significantly reduced. Anyhow, at the same time the mass was

increased for 75.8% (from 87 grams to 153 grams), which was unacceptable, indicating need to introduce additional parameters in the optimization process. Thus, three-parameter and later on, five-parameter optimization was performed, using models as described in the following text. Three-parameter optimization was done using two models, one of them already described in all necessary details in [32].

3.1. Model for Three-Parameter Lug Optimization

Model for three-parameter optimization had three geometrical input parameters: thickness (Fig. 5), rounding radius and the radius of a pin hole (Fig. 6). More details can be found in [24, 32].

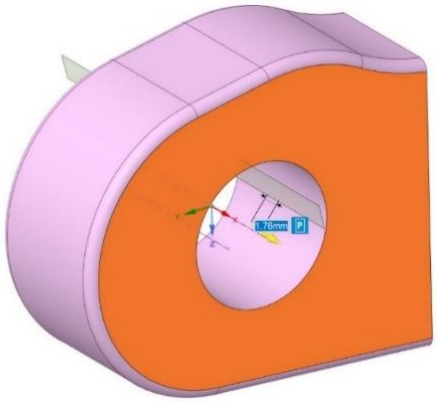

Fig. 5 Thickness modeling normal to the marked face [24]

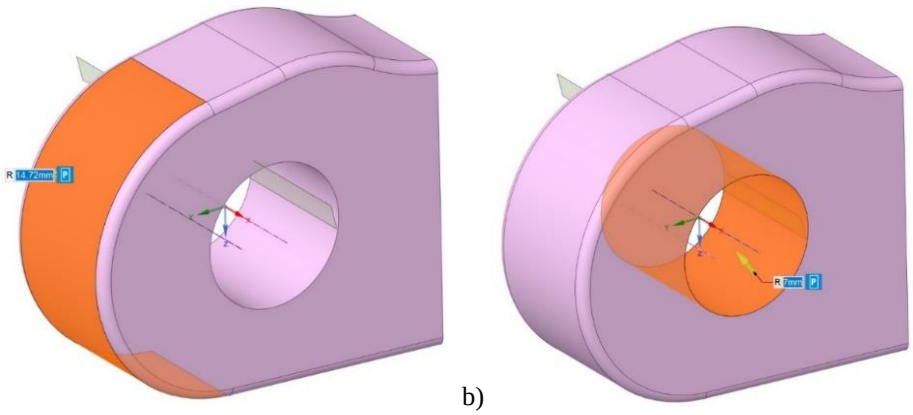

a) b)

Fig. 6 Radii of highlighted surfaces were varied: a) rounding radius, b) radius of pin hole

Two models were made for three-parameter optimization, one of them already described in [32]. In the second model, the initial lug thickness of 12 mm was kept the same, but the rounding radius was increased to 19 mm, whereas the pin hole radius was 7.5 mm. For this model, the mass was 105 grams and SIF values after the first crack

propagation step are over 1400 MPa√mm, Fig. 7a. The SIF values after crack growth of 7.09 mm are shown in Fig. 7b. Figure 8 shows the number of cycles for three-parameter model presented here and original lug model up to the crack length 7 mm (crack length reached almost 11 mm in the case of three-parameter model).

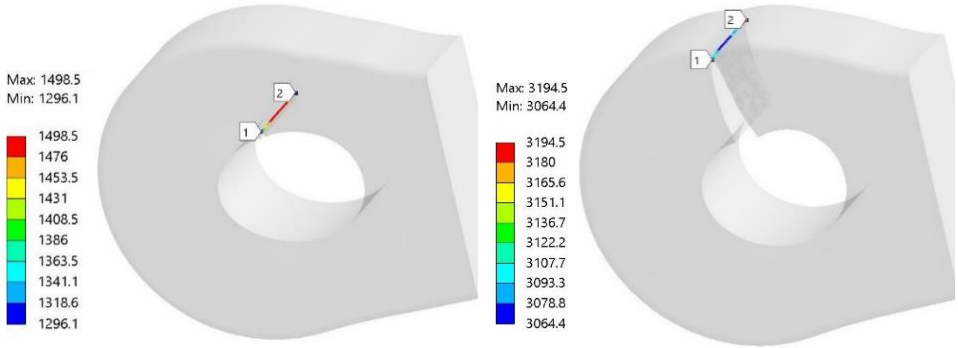

Fig. 7 SIF values along crack front after: a) 1st step of growth, b) 15th step of growth

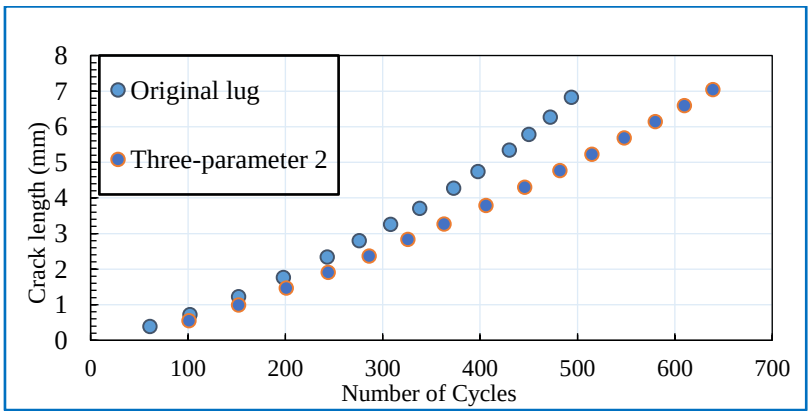

Fig. 8 Crack length vs Number of cycles for thee lug models

3.2. Models for Five-Parameter Lug Optimization

Two more parameters, shown in Fig. 9, were additionally varied to get five-parameter optimization. One of them, so-called pull up, Fig. 9a, was used to make a „hump“, while the second one, Fig. 9b, was in charge of the outer radius with initial value 1 mm, which was varied up to 3-5 mm.

Using the Ansys Workbench® (Design Exploration module, the total number of 31 design point were generated, three radii, pull up (hump) and thickness, with the initial combination marked in red, Fig. 10. Besides 5 input parameters, the resulting mass, as the output parameter, is shown in Fig. 10.

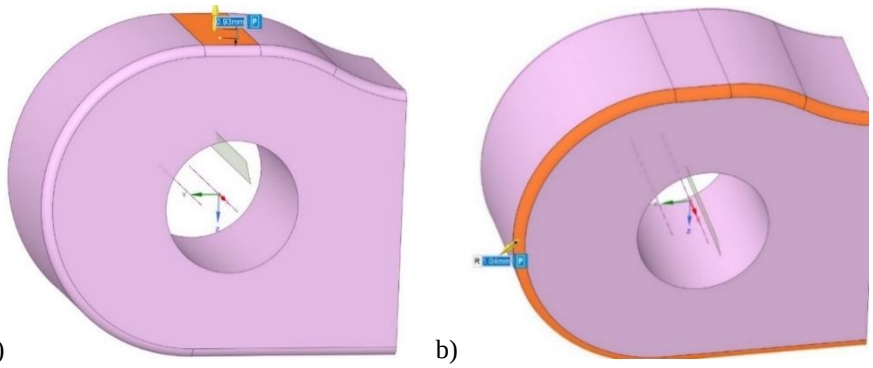

a) b)

Fig. 9 a) Hump parameter, b) Outer Radius

Table of Design Points

	A	B	C	D	E	F	G
1	Name	P3 - radius 1	P12 - radius 3	P13 - radius 4	P14 - add thickness	P15 - pull up	P6 - SYS-3\PartBody Mass
2	Units	mm	mm	mm	mm	mm	tonne
3	DP 1	16.94	1	1	3.29	0.55	0.00010123
4	DP 2	19	1	1	3.29	0.55	0.00015299
5	DP 6	11.331	1	1	3.29	0.55	
6	DP 7	11.331	1	1	3.29	0.55	
7	DP 10	17.669	1	1	3.29	0.55	
8	DP 11	17.669	1	1	3.29	0.55	
9	DP 13	14.5	1	1	3.29	0.55	8.5488E-05
10	DP 17	14.5	1	1	3.29	0.55	
11	DP 21	11.331	1	1	3.29	0.55	
12	DP 22	11.331	1	1	3.29	0.55	
13	DP 25	17.669	1	1	3.29	0.55	
14	DP 26	17.669	1	1	3.29	0.55	
15	DP 27	14.5	1	1	3.29	0.55	7.8377E-05
16	DP 28	16	3	3	2.961	0.55	7.8384E-05
17	DP 29	15.433	2.4333	2.4333	3.1968	0.56558	7.8384E-05
18	DP 30	15.433	2.4333	3.5667	3.1968	0.53442	7.8384E-05
19	DP 31	15.433	3.5667	2.4333	3.1968	0.53442	7.8384E-05
20	DP 32	15.433	3.5667	3.5667	3.1968	0.56558	7.8384E-05
21	DP 33	16.567	2.4333	2.4333	3.1968	0.53442	7.8384E-05
22	DP 34	16.567	2.4333	3.5667	3.1968	0.56558	7.8384E-05
23	DP 35	16.567	3.5667	2.4333	3.1968	0.56558	7.8384E-05
24	DP 36	16.567	3.5667	3.5667	3.1968	0.53442	7.8384E-05
25	DP 37	14	3	3	3.29	0.55	7.8384E-05
26	DP 38	16	1	3	3.29	0.55	7.8384E-05
27	DP 39	16	3	1	3.29	0.55	7.8384E-05
28	DP 40	16	3	3	3.29	0.495	7.8384E-05
29	DP 41	16	3	3	3.29	0.55	7.8384E-05
30	DP 42	17	3	3	6	2.3	0.00013859
31	DP 43 (Current)	16	3	3	3	4	0.00010653
32	DP 44	14.5	3	3	3	2.5	0.00010137
33	DP 45	17	1	1	3	4	0.00012141

Fig. 10 Generated design points

Figure 11 presents all parameters, including the stress intensity factor, as the second output parameter. Its values are given separately in the following text.

Outline of All Parameters

	A	B	C	D
1	ID	Parameter Name	Value	Unit
2	Input Parameters			
3	Static Structural (A1)			
4	P3	radius 1	16	mm
5	P12	radius 3	3	mm
6	P13	radius 4	3	mm
7	P14	add thickness	3	mm
8	P15	pull up	4	mm
*	New input parameter	New name	New expression	
10	Output Parameters			
11	Static Structural (A1)			
12	P6	SYS-3\PartBody Mass	0.00010653	tonne
13	P10	SIFS (K1) Maximum	1590.2	MPa mm^0.5
*	New output parameter		New expression	
15	Charts			

Fig. 11 Input and output parameters

Five models were made and used, with different input parameters providing different geometries, as shown in Fig. 12, together with the results for the distribution of stress intensity factors.

Based on values for the stress intensity factors, the number of cycles is calculated for all models and used to construct diagrams crack length vs. number of cycles, as shown in Fig. 13. Results are also shown in Table 1 for the initial value of K_{Imax} and total number of cycles.

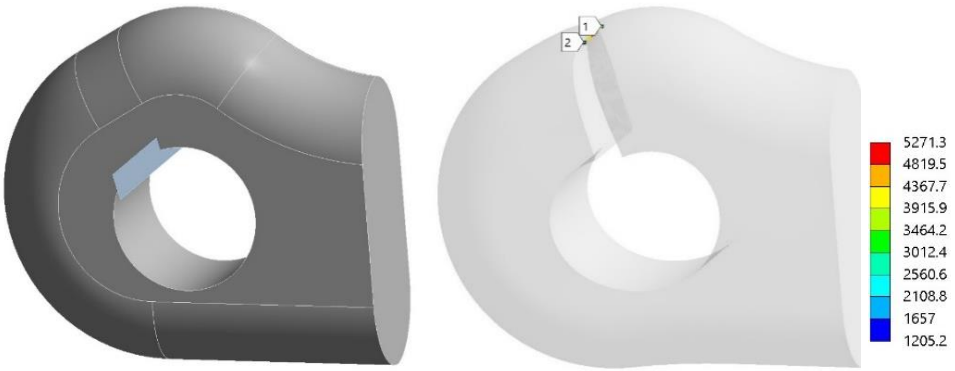

a) Model 1 – mass 80.7 g, SIF_{max} 5271.3 MPa√mm

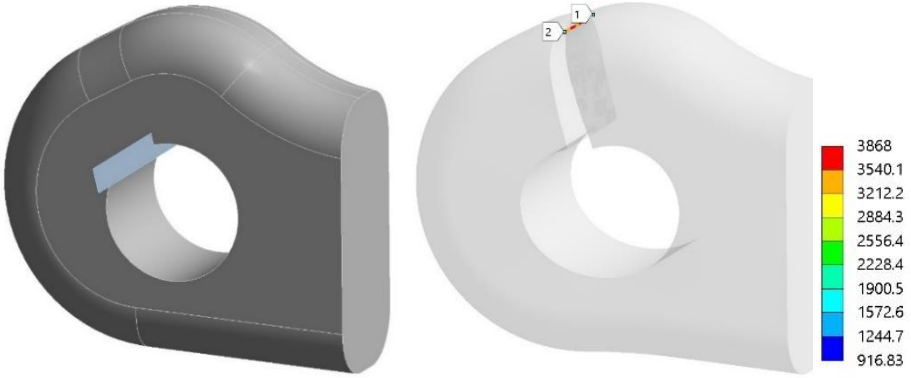

b) Model 2 – mass 87.6 g, SIFmax 3868 MPa√mm

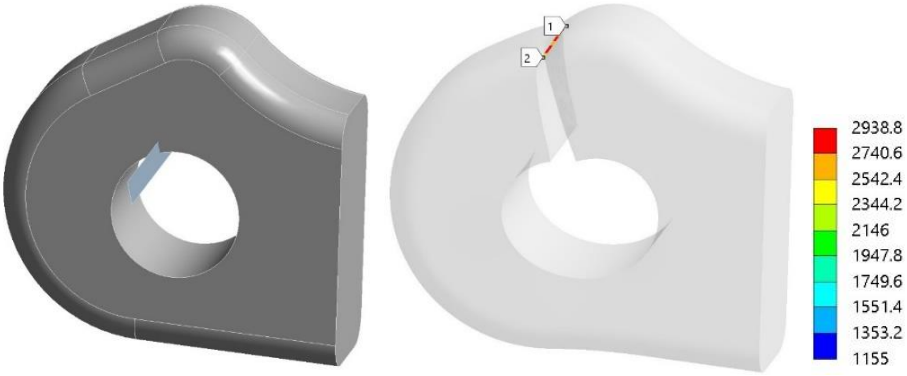

c) Model 3 – mass 97.4 g, SIFmax 2938.8 MPa√mm

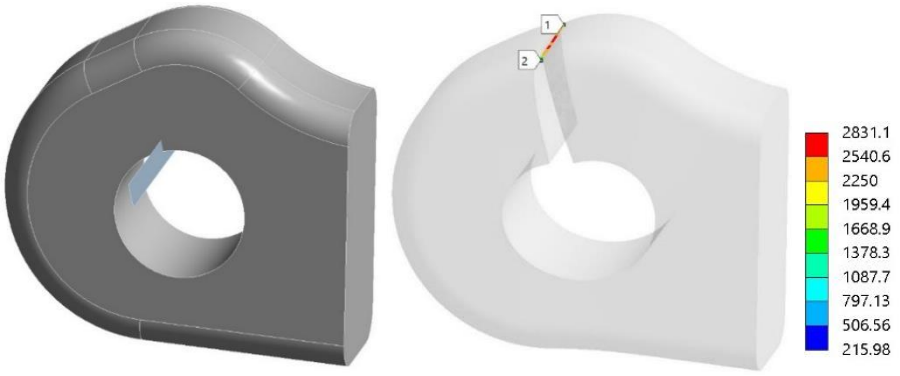

d) Model 4 – mass 100.1 g, SIFmax 2831.1 MPa√mm

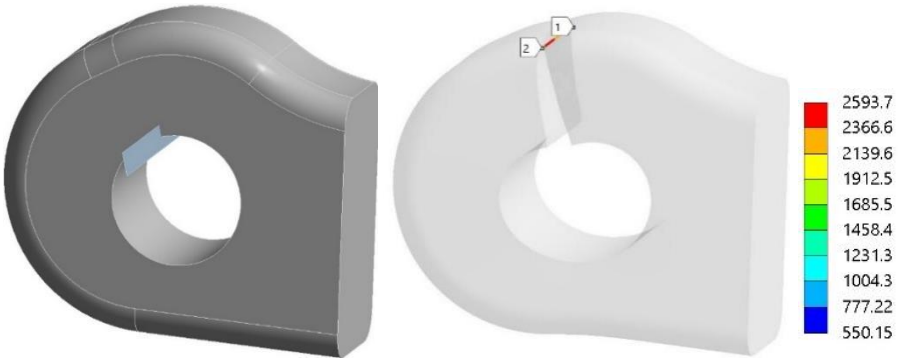

e) Model 5 – mass 106.5 g, SIF_{max} 2593.7 MPa√mm

Fig. 12 Five models for the five-parameter optimization

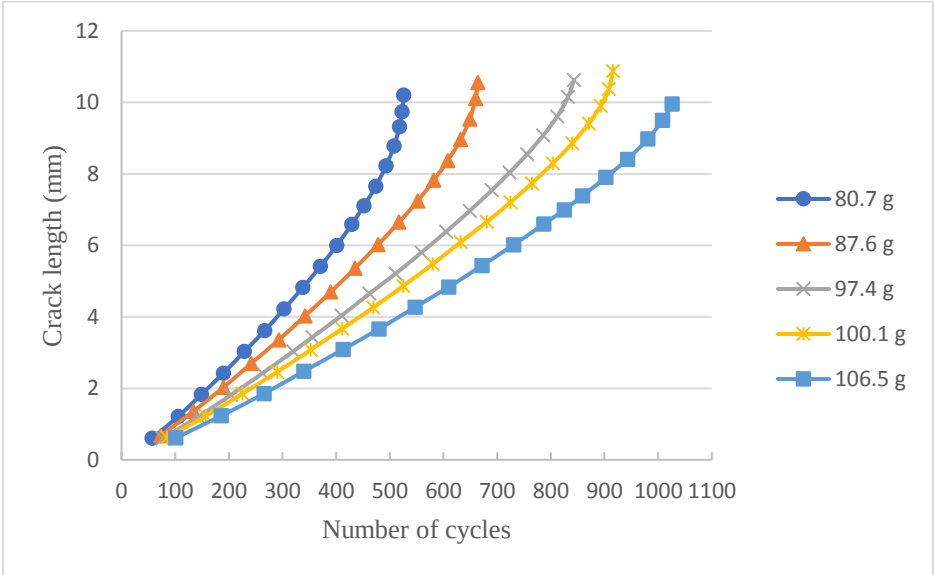

Fig. 13 Crack length vs. number of cycles for the five-parameter models

Table 1 Results for five-parameter models

	Mass (g)	Thickness (mm)	Initial K_{Imax} (MPa√mm)	Total Number of Cycles
Original lug	87	12	1880	515
Model 1	80.7 (-7.24%)	13	1883	526 (+2.1%)
Model 2	87.6 (+0.7%)	13	1788	664 (+28.9%)
Model 3	97.4 (+12%)	13.5	1641	843 (+63.7%)
Model 4	100.1 (+15.1%)	14	1580	916 (+77.9%)
Model 5	106.5 (+22.4%)	15	1479	1026 (+99.2%)

4. DISCUSSION

Table 1 indicates modest increase in mass and significant increase in fatigue life, generally speaking. In the case of model 1, mass is even reduced slightly, but increase in fatigue life is not remarkable. Model 2 has almost the same mass with increase of fatigue life close to 30%, while models 3-5 provide fatigue life increase 63.7-99.2% with increase of mass 12-22.4%, making them all candidates for practical use of presented optimization, especially since modern CNC machines can easily produce any of these shapes.

Comparison with Three-parameter optimization is clearly in favour of Five-parameter optimization, both regarding the first Three-parameter model, described in [28] and the second one, described here, since they provided smaller increases in life (52.6-60%) with larger increase in mass (20.7-24.1%). In other words, with approximate the same increase of mass (22.4% vs. 20.7%), increase of fatigue life is higher (99.2% for model 5) compared to 60% (Three-parameter, 2nd model).

One can see from Fig. 10 that the shape of a 'hump' affects the fatigue life, as well as the outer radius. For easier comparison, previous optimization options are summarized in Table 2, indicating the longest fatigue life in the case of the two-parameter optimization model (3.75 times), but at the cost of 75.9% of mass increase, [24]. On the other hand, model 5 (Table 1) results in a mass increase of only 22.4%, providing almost 2 times longer fatigue life, so it seems to be the optimal option. Anyhow, if the risk of failure is high, then the best option is the one with the highest number of cycles.

Table 2 Comparison of properties for five lug models

	Mass (g)	Initial K_{Imax} (MPa√mm)	Total number of cycles
Original lug	87	1880.0	515
Thickness 17 mm	123 (+41.4%)	1391.2	1085 (+110.7%)
Two-parameter	153 (+75.9%)	1256.8	1933 (+275.4%)
Three-parameter model 1	108 (+24.1%)	1267.6	786 (+52.6%)
Three-parameter model 2	105 (+20.7%)	1498.5	824 (+60.0%)

At this point, it is important to clarify and distinguish between two design principles, safe-life vs. fail-safe. In the first case, cracks are not accounted for, since the essence of safe-life principle is to assure full design life of a component without cracks. Optimization in that case is meaningless since its aim is to increase number of cycles from the initial to the critical crack length. i.e. to increase life of a cracked component. On the other side, fail-safe principle enables safe operation of a cracked component if fatigue crack growth rate is such that the critical crack length is not reached before the next NDT testing. For this approach one needs reliable experimental data for fatigue crack growth rate and realistic numerical simulation of fatigue crack growth, as demonstrated here.

Finally, one should keep in mind eventual effect of Paris coefficients, C and m, and problems with their evaluation. The best option would be to test material in the standard way, [33], under the conditions as close to real ones as possible, but that was not an option here. Any other experimental data, like dependence between crack length and number of cycles, could be also use to calibrate C and m, but that was not an option here as well. Therefore, we had to rely on database available in literature.

5. CONCLUSIONS

Based on the results presented in this paper, one can conclude the following:

- The longest fatigue life in the scope of Five-parameter optimization is obtained with model 5 (99.2%) with modest increase of the mass (22.4%). More complex shape of model 5 is not a problem, since modern CNC machines can easily produce it.
- Compared with others, the Five-parameter model 5 provides the best option, unless the longer fatigue life is the only criterion.
- Optimization of attachment lug significantly improves fatigue life and thus, reduces the risk of failure, so it fits well in the fail-safe design approach. At the same time, mass is increased, but not significantly.
- Numerical simulation of the fatigue crack growth, if verified and applied in an appropriate way, is the best option to improve design and safety of critical airplane components.

REFERENCES

1. Grbović, A., Solob, A.Y., Sedmak, S., Sedmak, A., 2023, *Numerical and experimental analysis of the integrity of light aircraft wing structure*, Structural Integrity and Life, 23(2), pp. 167-172.
2. https://sassofia.com/blog/considerations-related-to-faa-supplemental-structural-inspection-programme-ssip/ (last access 26.06.2024)
3. *Boeing's latest crisis is growing after an airline found cracks on two 737 planes that weren't due for inspection yet*, https://www.businessinsider.com/boeing-737ng-pickle-fork-crack-lion-air-2019-11. (last access 26.06.2024)
4. https://www.theguardian.com/business/2019/nov/06/boeing-737-cracks-ryanair-grounds-three-planes-due-to-cracking-between-wing-and-fuselage. (last access 26.06.2024)
5. Braga, D.F.O., Tavares, S.M.O., da Silva, L.F.M., Moreira, P.M.G.P., de Castro, P. M.S.T., 2014, *Advanced design for lightweight structures: Review and prospects*, Progress in Aerospace Sciences, 69, pp. 29-39.
6. Solob, A.Y., 2021, *Fatigue life analysis of damaged light aircraft wing fuselage fitting*, Ph.D. Thesis, University of Belgrade, Faculty of Mechanical Engineering.
7. Barter, S., Sharp P.K., Clark, G., 1994, *The failure of an F/A-18 trailing edge flap hinge*, Engineering Failure Analysis, 1(4), pp. 255-266.
8. Witek, L., 2006, *Failure analysis of the wing-fuselage connector of an agricultural aircraft*, Engineering Failure Analysis, 13(4), pp. 572-581.
9. Azevedo, C.R.F., Hippert Jr, E., Spera, G., Gerardi, P., 2002, *Aircraft landing gear failure: fracture of the outer cylinder lug*, Engineering Failure Analysis, 9(1), pp. 1-15.
10. Huang, X., Moan, T., 2007, *Improved modeling of the effect of R-ratio on crack growth rate*, International Journal of fatigue, 29(4), pp. 591-602.
11. Lanciotti, F. Nigro, Polese, C., 2006, *Fatigue crack propagation in the wing to fuselage connection of the new trainer aircraft M346*, Fatigue Fract Eng Mater Struct., 29(12), pp. 1000-1009.
12. Wu, L.M., He, Y.T., Zhang, H.W., Cui, R.H., Du, J.Q., Ding, H., 2011, *Study on fatigue crack growth model of attachment lug subjected to oblique pin-load*, Advanced Materials Research, 291-294, pp. 1043-1050.
13. Sumanth, T.A.M.H., 2018, *Comparative analysis of aircraft wing fuselage lug attachment bracket*, International Journal for Technological Research in Engineering, 5(11), pp. 4422-4429.
14. Shridhar, K., Suresh, B.S., Kumar, M.M., 2019, *Fatigue Analysis of Wing-Fuselage Lug section of a Transport Aircraft*, Procedia Structural Integrity 14, pp. 375-383.
15. Rigby, R., Aliabadi, M. H., 1997, *Stress intensity factors for cracks at attachment lugs*, Engineering Failure Analysis, 4(2), pp. 133-146.
16. Kim, J.-H., Lee, S.-B., Hong, S.-G., 2003, *Fatigue crack growth behavior of Al7050-T7451 attachment lugs under flight spectrum variation*, Theoretical and applied fracture mechanics, 40(2), pp. 135-144.

17. Maksimović, M., Vasović, I., Maksimović, K., Trišović, N., Maksimović, S., 2018, *Residual life estimation of cracked aircraft structural components*, FME Transactions, 46(1), pp. 124-128.
18. Boljanovic, S., Maksimovic, S., 2014, *Fatigue crack growth modeling of attachment lugs*, International Journal of Fatigue, 58, pp. 66-74.
19. Boljanović, S., Maksimović, S., 2017, *Fatigue damage analysis of wing-fuselage attachment lug*, Procedia Structural Integrity, 5, pp. 801-808.
20. Antoni, N., Gaisne, F., 2011, *Analytical modelling for static stress analysis of pin-loaded lugs with bush fitting*, Applied Mathematical Modelling 35(1), pp. 1-21.
21. Mookaiya, K., Balaji, S., Balakrishan, S.R., 2013, *Crack Growth Analysis in Aircraft Wing Lug Section and Fatigue Life Estimation*, International Journal of Engineering Research and Technology, 2(6), pp. 2018-2023.
22. Naderi, M., Iyyer, N., 2015, *Fatigue life prediction of cracked attachment lugs using XFEM*, International Journal of Fatigue, 77, pp. 186-193.
23. Solob, A., Grbović, A., Božić, Ž., Sedmak, S.A., 2020, *XFEM based analysis of fatigue crack growth in damaged wing-fuselage attachment lug*, Engineering Failure Analysis, 112, 104516.
24. Grbović, A., Solob, A.Y., Sedmak, S., Sedmak, A., 2023, *Optimization of wing-fuselage attachment lug*, Structural Integrity and Life, 23(2), pp. 161-165.
25. Grbovic, A., Solob, A., Bozic, Z., Sedmak, S., Sedmak, A., 2024, *Fatigue life of damaged wing-fuselage fitting*, Procedia Structural Integrity 58, pp. 42-47.
26. Sedmak A. 2024, *Fatigue crack growth simulation by extended finite element method: A review of case studies*, Fatigue Fract Eng Mater Struct., e14277.
27. Li, H., Li, J., Yuan, H., 2018, *A review of the extended finite element method on macrocrack and microcrack growth simulations*, Theoretical and Applied Fracture Mechanics, 97, pp. 236-249.
28. Martínez, E.R., Chakraborty, S., Tesfamariam, S., 2021, *Machine learning assisted stochastic-XFEM for stochastic crack propagation and reliability analysis*, Theoretical and Applied Fracture Mechanics, 112, 102882.
29. *SMART Fracture Whitepaper*, available at: https://www.ansys.com/resource-library /white-paper/smart-fracture. (last access 27.06.2024)
30. Grbović, A., Sedmak, A., Lazić-Vulićević, Lj., Zaidi, R., Kirin, S., 2023, *Extended finite element method simulation of fatigue crack growth in Charpy specimen*, Structural Integrity and Life, 23(3), pp. 237-242.
31. Busari, Y.O., Manurung, Y.H.P., 2020, *Welded high strength low alloy steel influence on fatigue crack propagation using LEFM, a practical and thematic review*, Structural Integrity and Life, 20(3), pp. 263-279.
32. Grbović, A. Solob, A., Sedmak, S. Sedmak, A. Božić, Ž., 2024, *Three-parameter optimization of an attachment lug*, Structural Integrity and Life, 24(1), pp. 124-127.
33. ASTM E647-23a, *Standard Test Method for Measurement of Fatigue Crack Growth Rates*, 2023.